



# Integration of microfluidics in smart acoustic metamaterials

Krishnadas Narayanan Nampoothiri<sup>1</sup>, Shubhi Bansal<sup>2,a</sup> , Abhishek Jha<sup>1</sup>, and Prateek Mittal<sup>2,b</sup>

<sup>1</sup> Department of Mechanical Engineering, Amrita School of Engineering, Amrita Vishwa Vidyapeetham, Chennai 601103, India

<sup>2</sup> Department of Computer Science, University College London, London, UK

Received 10 February 2023 / Accepted 2 February 2024  
© The Author(s) 2024

**Abstract** Microfluidics has achieved a paradigm-shifting advancement in life sciences, automation, thermal management, and various other engineering streams. In recent years, a considerable amount of research has been conducted on the use of microfluidics in designing novel systems and fabricating next-generation smart materials that are capable of outperforming historical barriers and achieving unprecedented qualities. One such innovative development is the integration of fluidics into building artificially structured smart materials called acoustic metamaterials to achieve active tunability for a real-time controllable manipulation of acoustic waves. Leveraging the capability of microfluidics to automate the manipulation of liquid droplets, fluid streams, or bubbles in a required arrangement has revolutionised the development of actively tunable fluidics-integrated acoustic metamaterials for widescale applications. This review first discusses the prominent microfluidic actuation mechanisms used in the literature to develop fluidics-integrated smart acoustic metamaterials, and then it details integrated metamaterial design and extraordinary applications such as active acoustic wave manipulation or building tunable acoustic holograms etc. The following review concludes by providing the importance and future perspective of integrating microfluidic techniques with novel metamaterial designs, paving the way for innovative futuristic applications.

## 1 Introduction

Microfluidics is the science which studies the behaviour of fluids in microscale regimes and allows the manipulation of tiny volumes of fluids from microliter ( $\mu\text{l}$ ) to femtolitre (fl) range, which holds immense potential in various industrial areas like pharmaceutical, biomedical, and microelectronics [1, 2]. Various microfluidic techniques utilising controlled liquid and droplet manipulations have been integrated with lab-on-chip and point-of-care diagnostic devices for the betterment of society [3–5]. Microfluidics allows to develop of reliable and accurate devices at microscale regimes by dealing with viscous and surface tension forces and larger surface-to-volume ratios which are dominant in microscale regimes when compared to liquid handling in the macroscale regime. These unique features have been widely exploited and led to the development of novel techniques like 3D printing [6], food-borne disease detection [7], pathogen detection [8], drop impact printing [9], and sorting of cells [10].

Recently, researchers have started exploring the capability of microfluidics to integrate and fabricate the next-generation smart materials to achieve unprecedented qualities that were not possible before using the conventional materials. One such emerging smart material field where microfluidics has demonstrated extraordinary capabilities is metamaterials. In general, metamaterials are specially designed artificially structured materials, possessing extraordinary properties like negative mass density, negative refractive index, zero bulk modulus etc. [11]. Negative mass density is one such property that enables metamaterials to repel objects as if they have an opposite mass density [12]. This can be useful in areas like propulsion and levitation [13–15]. Another property of metamaterials is the negative refractive index, which enables them to bend waves, such as sound or light waves, in unusual ways,

Krishnadas Narayanan Nampoothiri and Shubhi Bansal Equal contribution joint first authorship.

<sup>a</sup> e-mail: [shubhi.bansal@ucl.ac.uk](mailto:shubhi.bansal@ucl.ac.uk) (corresponding author)

<sup>b</sup> e-mail: [prateek.mittal@ucl.ac.uk](mailto:prateek.mittal@ucl.ac.uk) (corresponding author)

making it possible to create lenses that are much thinner than conventional lenses [16]. These lenses can be useful in applications like microscopy and imaging [13, 17]. Zero bulk modulus is another property of metamaterials that allows them to deform in unusual ways when subjected to stress, which can be used to create materials that are extremely flexible and can be stretched or compressed in ways that are not possible with the conventional materials [15, 18]. Depending on the properties of metamaterials, they are used to manipulate electromagnetic, acoustic, or thermal waves [19], which leads to further classification of the type of metamaterials as electromagnetic metamaterials [20], acoustic metamaterials [21–23] and so on. An extensive amount of research has been done by integrating microfluidics with electromagnetic metamaterials to achieve tunability [24–27]. Various novel metamaterials like meta-fluidic metamaterial [19] and liquid crystals [20, 28] have been developed with this new amalgamation to outperform the conventional electromagnetic metamaterials. On the other hand, acoustic metamaterials (AMMs) deal with manipulating sound waves and have been progressively researched to overcome the limitations of conventional materials like poor reconfigurability, low tunability, etc. [21, 29–31]. Acoustic metamaterials have been utilised for a wide range of applications in various fields [32]. For example, they are being used as sound barriers for curbing sound pollution in urban areas [33]. Acoustic metamaterials have also found profound applications in medical imaging and non-destructive testing to focus sound waves [34, 35] as well as to create cloaking devices that make objects invisible to sound waves [31]. Moreover, vibration control is another area where acoustic metamaterials have been utilised to absorb or redirect vibrations and thus protect structures from natural disasters [30, 36]. Additionally, sensors that detect sound waves and vibrations can also be created using acoustic metamaterials, thus finding potential applications in structural health monitoring [37, 38]. To address these issues, researchers have recently started investigating the integration of microfluidics with acoustic metamaterials to achieve extraordinary capabilities. In this review, we focus on acoustic metamaterials utilising fluidic manipulation to achieve active acoustic tunability, which leads to synergistic convergence of microfluidics and acoustic metamaterials, enabling numerous varied applications.

The paper is organized as follows: Sect. 2 describes the relevant microfluidic domains utilised in building the acoustic metamaterials, which is followed by limitations of conventional acoustic metamaterials in Sect. 3. Section 4 reviews the fluidics-integrated acoustic metamaterials and their prominent applications. Section 5 concludes the study with futuristic directions and perspectives.

## 2 Relevant microfluidic domains

Microfluidics can be categorised into multiple domains depending upon the manipulation and control of fluid as droplets, bubbles, or continuous liquid streams with finite flow rates. This section provides an overview of the key microfluidic domains utilised in developing integrated AMMs.

### 2.1 Digital microfluidics (DMF)

DMF is a microfluidic domain where liquids are manipulated as discrete droplets for various integrated microfluidic applications [39]. Either the droplets are placed on the planar chips using pipettes, or they are created from a liquid pool [40] using various external forces such as electric forces [41] and magnetic forces [42]. These forces are also responsible for further droplet manipulations, such as droplet splitting [43], droplet transportation [44], droplet bouncing [45] and droplet merging [46]. DMF offers flexibility in functioning multiplex and parallel operations [47], researchers prefer this domain for developing microfluidic devices, especially for lab-on-chip applications [48]. Metal deposition, photolithography, and subsequent etching are the most common processes used for fabricating such devices [49, 50]. Apart from electric forces, there are systems which rely on magnetic force [51], as well as acoustic force [52]. These DMF techniques are used for demonstrating integrated microfluidic platforms [53], with biochemical detection methods [54], for developing sensors [55–57], label-free optics [58, 59], and mass spectrometers [47, 60].

### 2.2 Continuous flow microfluidics (CFM)

In CFM, manipulation of liquid flow takes place through the fabricated microchannels [61]. The flow rates of the liquid will be in the range of  $\mu\text{l}/\text{min}$ . Fluid flow is established by external units, such as micropumps and syringe pumps, or by integrated internal mechanisms, such as electric, magnetic, and capillary forces. In this domain, microchannels are fabricated using the standard fabrication techniques like photolithography [62] and soft lithography [63]. This domain finds applications in biology [64], chemistry [65], and several other areas for separating micro/nanoparticles [66], cell sorting [67], as well as for pathogen detection [68].

### 2.3 Bubble based microfluidics (BM)

In recent years, researchers have started working in a new microfluidic domain, which is based on the manipulation of bubbles [69]. Microbubbles can be generated using various methods, such as electrolysis [70], heating [71], trapping techniques [72], and through injection [73]. Since microbubbles can be easily produced and removed after their assigned tasks, BM has offered a new paradigm in integrating microfluidics with different areas due to their unique property of specific responses to different energy sources and gas–liquid interactions [74], especially in handling biological targets [75, 76].

With the development of various microfluidic domains in recent years [77], extensive research has been aligned on developing and implementing microfluidics in designing novel systems and fabricating next-generation smart materials. One such innovative area is the integration of fluidics with metamaterials [78]. We bestow a perspective on acoustic metamaterials made by a blend of liquid and solid structures designed to enable extraordinary properties like on-demand sound wave modulation and active tunability. In the next section, we will review and discuss some of the key findings in this field.

## 3 Limitations of conventional acoustic metamaterials

Despite showing their enormous potential in varied application spaces, conventional acoustic metamaterials are mostly passive, which implies that they have a fixed structure, resulting in a fixed operational functionality. Moreover, some of the conventional metamaterials have structure-centric limitations that can hinder their performance in certain applications [30]; for example, the periodic microstructures of acoustic metamaterials embedded within a matrix material are often limited to a small frequency range (near the resonance frequency), and their operating bandwidths are narrow [31], thereby limiting their applications. Some of the acoustic metamaterials are also sensitive to changes in the environment, such as temperature and humidity, which thereby can affect their performance for being used in various applications [11, 32, 38]. In the last decade, tunable acoustic metamaterials have been proposed to overcome the limitations of passive metamaterials and to allow multiple functionalities by tuning the structure of the metamaterial using electrical, magnetic, or other actuation mechanisms. But still, the complex fabrication process, as well as the difficulty in scaling up to larger sizes, hinders metamaterial's practical applications [29].

## 4 Fluidics-integrated acoustic metamaterial designs

In one of the pioneering works, Tian et al. [79] have reported a programmable acoustic metasurface using a combination of a fluidic channel with five shunted Helmholtz resonators. Helmholtz resonator is a device that consists of a rigid container with a small neck and a hole on one end and a larger hole on the other end to emit sound. When air is forced into the container, the pressure inside increases [80]. When the external force pushing the air into the container is removed, the higher-pressure air inside will flow out. Due to the inertia of the moving air, the container will be left with a pressure slightly lower than the outside, causing air to be drawn back in. This process repeats, with the pressure oscillations increasing and decreasing asymptotically after the sound starts and stops. The resonant mass of air in the container is set in motion through the second, larger hole, which does not have a neck. Helmholtz resonators play a pivotal role in constructing acoustic metamaterials [79, 81]. By utilising Helmholtz resonators in metamaterials, certain functionalities like sound absorption, waveguiding, and focusing of sound waves in certain directions can be achieved. Tian et al. [79] showed the strategic combination of the Helmholtz resonator with fluid channels, where the cavity size is tuned by pumping liquid in/out through the channel (as shown in Fig. 1(A (i))). The unit cell has dimensions of  $h_1 = 21$  mm,  $h_2 = 1$  mm,  $h_3 = 2.5$  mm,  $h_4 = 7$  mm,  $w_1 = 6.2$  mm,  $w_2 = 1.5$  mm, and  $w_3 = 1.8$  mm, which can be seen in Fig. 1(A (ii)). The width of each unit cell is 27.8 mm, roughly a quarter wavelength (28.6 mm) at the frequency of interest (3.0 kHz), so it provides adequate spatial resolution. The fluid volume in the resonator can be adjusted easily using a robust fluidic system to control the cavity size (or height  $h_1$ ). This allowed the meta-cell (i.e., an individual unit of the metasurface, which repeats itself to create a full metasurface) to manipulate the phase of the transmitting wave in the sub-wavelength scale (3.0 kHz) and achieved  $2\pi$  phase modulation by pumping 12 mL of water out of the cavities in 24 s. With this development, various applications of acoustic wave steering, acoustic beam engineering, and switching ON/OFF acoustic energy flow have been attained which was not achievable before using conventional passive Helmholtz resonators. The integration of liquids provide the advantages of active tunability through liquid volume, position and shape control, which are extremely difficult to achieve using solid structures.

In another work, Bansal and Subramanian [82] applied a concept of DMF-based EWOD technique to develop a microfluidic acoustic metamaterial (MAM). Here, an aperture or slit-type metamaterial was integrated with a

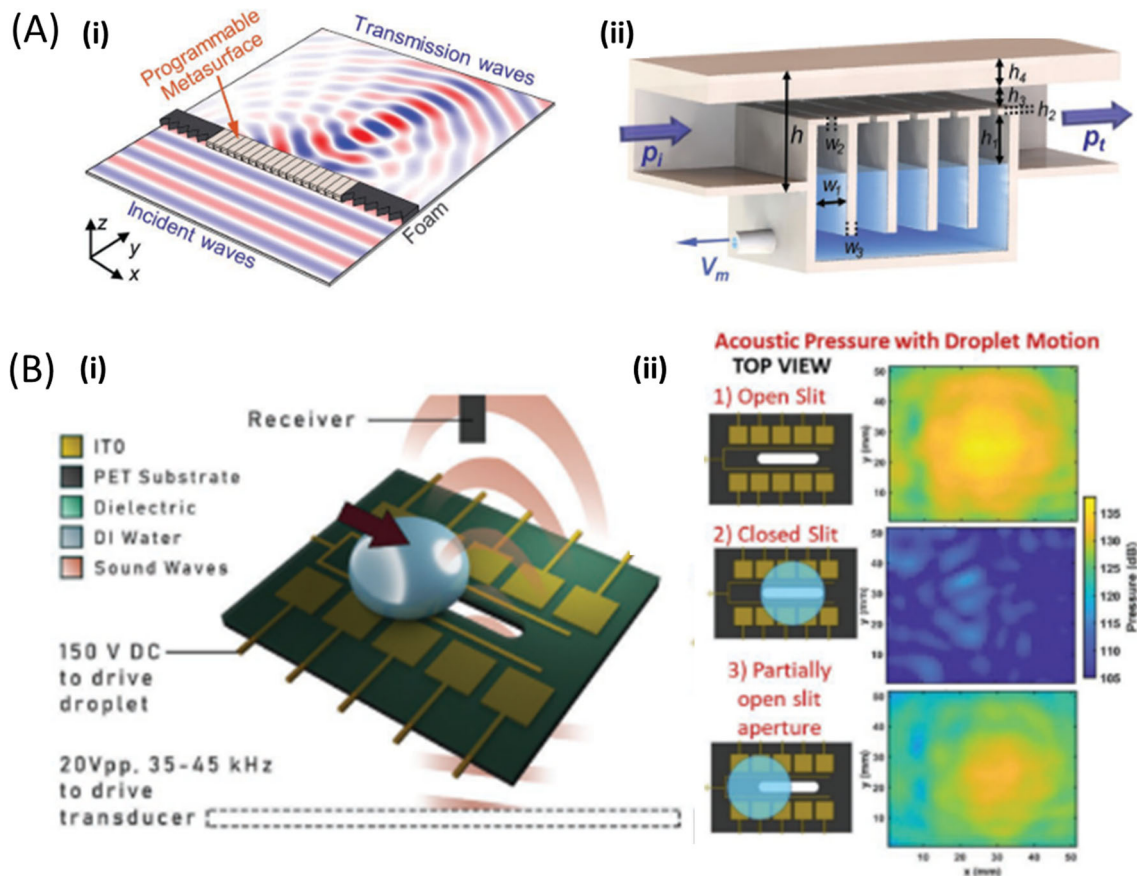


**Fig. 1** **A** (i) A schematic illustration of a programmable acoustic metasurface to manipulate acoustic waves. (ii) Representation of a unit cell of the metasurface, which is tuned by changing fluid volume to modulate the response of five shunted Helmholtz resonators [79]. **B** (i) A geometrical description of a microfluidic acoustic metamaterial (MAM) comprising a liquid droplet moving over a sub-wavelength slit using the EWOD technique. (ii) Representation of the top-view of the MAM with different droplet positions and the corresponding measured acoustic pressure maps for 40 kHz ultrasound [82]

movable water liquid droplet, which was moved over the slit to tune its open aperture length, as shown in Fig. 1(B (i)). This work talks about moving a droplet over a slit, i.e., a deep sub-wavelength opening (dimensions, length =  $0.5 \lambda$  (L), width =  $0.06 \lambda$ , and height =  $0.02 \lambda$ ) in a substrate for manipulating ultrasound (40 kHz, implying  $\lambda = 8.66$  mm) as shown in Fig. 1(B (ii)). The high impedance of the droplet's water–air interface blocked the transmitting sound field, thus altering the phase and amplitude of transmitting sound waves through variable aperture length. The acoustic applications of actively tunable switching, acoustic phase and amplitude modulation were demonstrated through this MAM design. Here, water droplets have been used as an integral part of acoustic metamaterials to provide an unexpected level of tunability and reconfigurability to manipulate acoustic fields.

Alongside the liquid channels and the liquid droplets, microfluidic arrays of bubbles have enabled a new paradigm for acoustic wave manipulation. Recently, 3D soft acoustic metamaterials were reported using bubbles as resonator units to manipulate acoustic waves [83]. In this study, a 3D bubble array was prepared by immersing a 3D-printed hydrophobic frame in water for manipulating sound waves for futuristic applications like negative refractive index metamaterials and acoustic super-lenses in a water environment (Fig. 2(A (i)). For each sample, each edge of the cubic frame has a cylinder shape with radius  $r$ . The cubic frame has a length of  $d$  and a lattice length of  $L$ , which remains constant in all three directions. The geometric parameters are selected as  $d = 3$  mm,  $r = 0.75$  mm, and  $L = 10$  mm for the robust design that is suitable for acoustic measurements. However, by placing additional pillars in each face, the larger cubic bubbles of sizes 5, 7.5, and 10 mm, respectively, are achieved, as shown in Fig. 2(A (ii)). Figure 2(A (iii)) shows a large 3D-printed sample with five layers of bubbles, which is used in the acoustic transmission measurement. The scale bar is 5 cm.

Microbubble-based AMM surfaces have also been developed by electrolysis of the liquid using a targeted light pattern (Fig. 2(B)) [84]. A light projection of optical wave with a low intensity of  $65 \text{ mWcm}^{-2}$  was used to modify the acoustic waves wavefront to generate acoustic patterns like multiple foci within the frequency range of 100 kHz to 10 MHz. Here, the light source was a 532 nm laser beam, which was expanded and directed on a digital mirror



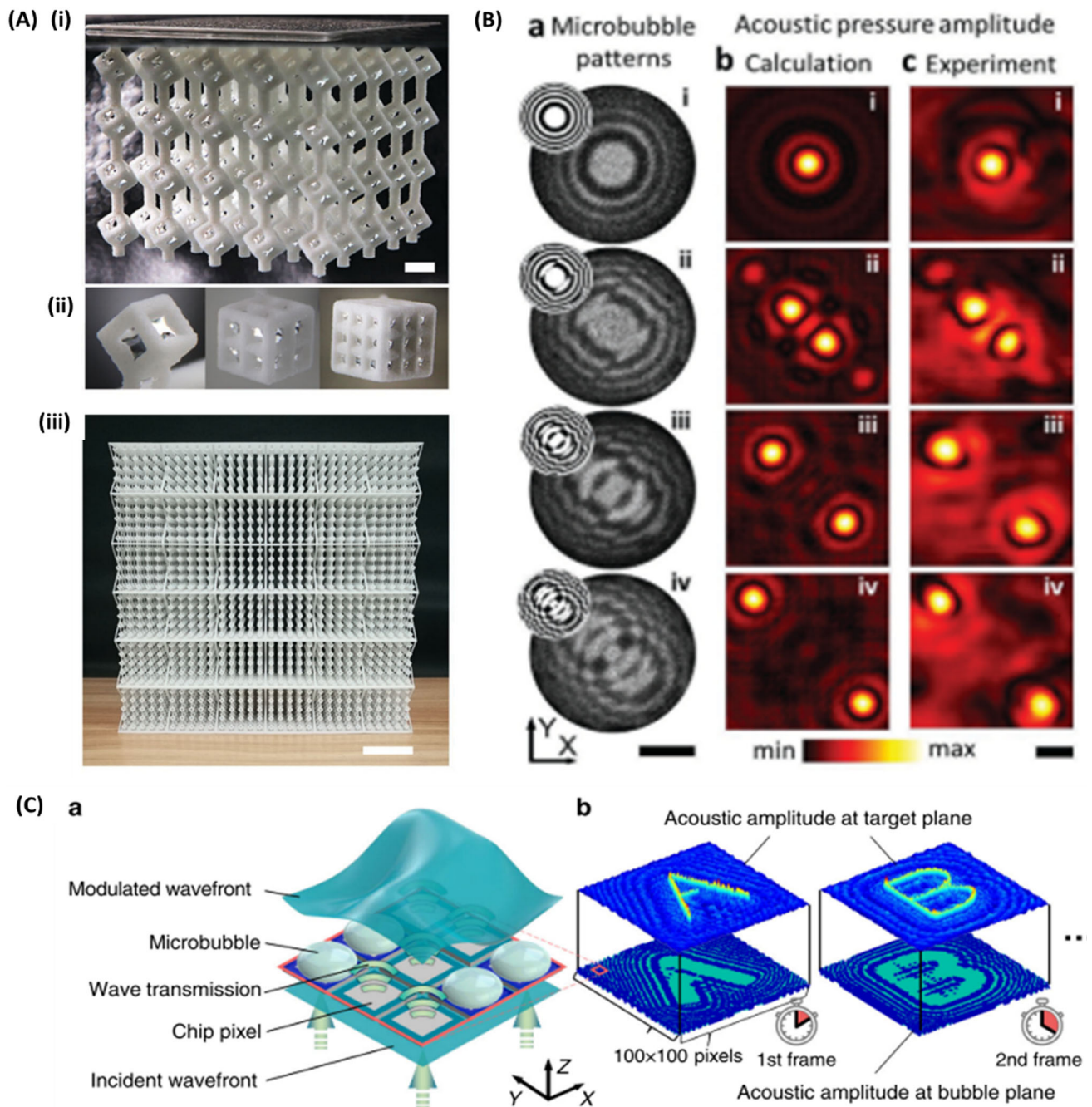


**Fig. 2** **A** Illustration of 3D-printed bubble array metamaterial designs [83]. **B** Schematic of the light addressed microbubble generation for acoustic field patterning [84]. **C** Representation of the spatial ultrasound modulation using microbubble patterns to encode the binary amplitude hologram of the target acoustic field [85]

device (DMD). DMD had an array of 1024 by 768 mirrors (pixels), which selectively reflected the light beam into patterns according to a software input. The reflected light pattern was then directed to the silicon wafer with a 45° angle of incidence to locally control the wafer’s electrical conductivity. The projection area on the wafer surface was  $29 \times 29 \text{ mm}^2$ , corresponding to 432 by 306 elements at the DMD. Every pixel (micromirror) of the optical modulator illuminated an area of  $67 \mu\text{m}$  by  $95 \mu\text{m}$  on the Si wafer. Within this area, many microbubbles were generated with differing sizes so that the optical pixel size did not correspond to the microbubble size.

Additionally, a digitally controlled microbubble array that could effectively and dynamically modulate the ultrasound field spatially was demonstrated, as shown in Fig. 2(C) [85]. Here, a thin layer of electrolyte liquid was placed between the conveyor film and the surface of a CMOS chip. The chip had 10,000 gold pads, each

measuring  $70\ \mu\text{m}$  by  $70\ \mu\text{m}$  and arranged in a  $100\text{-}\mu\text{m}$  by  $100\text{-}\mu\text{m}$  grid. An adjacent copper electrode served as the anode. By switching on a DC power supply, a potential difference was created between the copper electrode (+ 5 V) and the 10,000 gold electrode pads on the CMOS chip. This caused the surrounding water solution to undergo electrolysis, producing hydrogen and oxygen gases at the gold and copper electrodes, respectively. The size of the resulting microbubbles was controlled by regulating the current flow. The dynamic spatial ultrasound modulator (SUM) reshaped the incident plane acoustic waves into complex acoustic images using a digitally generated pattern of microbubbles controlled through a complementary metal–oxide–semiconductor (CMOS) chip, thus, showing a tunable approach toward acoustic holography. Active manipulation of a solid structure in millimetre or micron space (for developing kHz or MHz AMM, respectively) requires either electric or magnetic control on a sub-wavelength scale, which limits the individual functionality of each unit or meta-cell of a periodic AMM and increases the complexity of designing and fabricating an AMM. However, the microbubbles-based system has successfully demonstrated active kHz and MHz AMMs using microfluidic approaches at micron-scale regime. Thus, integrating microfluidics provides a new realm for developing more innovative, sub-wavelength, and actively tunable acoustic metamaterials.

Some other works have also utilised a water–air interface impedance to design a metasurface for manipulating sound waves. A trapped-bubble-based acoustic metamaterial has been theoretically investigated to predict its resonant behaviour for optimal performance [86] in varied applications like soundproofing, blast mitigation, and many others. Moreover, a bubble metascreen consisting of a single layer of gas inclusions in a soft solid was modelled as an open acoustic resonator to achieve acoustic super-absorption over a broad frequency range [87]. The bubble-based designs generally utilise bubbles as resonating scatterers to manipulate acoustic waves, and similarly, a bubbly diamond metamaterial utilised scattering by a periodic assembly of air bubbles for three-dimensional acoustic lensing [88].

While the designs mentioned above utilise the high impedance of the water–air interface for acoustic transmission, some metamaterials have also targeted the reverse. Recently, a tunable fluid-type acoustic metasurface (FAM) was developed for wide-angle and multifrequency water–air acoustic transmission [89]. FAM demonstrated a transmission enhancement of music signal across the water–air interface, which can be useful for applications like communicating between the ocean and atmosphere and other acoustic communications. Recently, a lotus leaf was also reported as a natural low-cost acoustic transmission metasurface, named a lotus acoustic metasurface (LAM), that demonstrates a wide-angle water-to-air acoustic transmission. An artificial acoustic metamaterial was designed based on the lotus effect by utilising superhydrophobic fabrication technologies to enable various promising applications in future, like detecting and imaging underwater objects from the air hydroacoustic and oceanography [89].

Rheological fluids [90], namely electro-rheological fluids (ERFs) [91] and magneto-rheological fluids (MRFs) [92], have also been considered as an active control medium for microfluidic droplets and to develop tunable acoustic metamaterials. ERFs change their viscosity and stiffness properties in response to an applied electric field, while on the other hand, MRFs change their stiffness in response to a magnetic field [93]. By distributing these fluids within the unit cell, researchers were able to modify the effective mass density and bulk modulus properties of the metamaterial, allowing for the control and manipulation of acoustic wavefronts [94, 95].

Since tunable acoustic metamaterials show enormous proficiencies in controlling sound waves in sub-wavelength-sized devices [93, 96], the integration of rheological fluids with fluidics-integrated acoustic metamaterials promises to deliver immense potential applications. Recent research has focused on developing self-regulating acoustic metamaterials that can autonomously adapt to changes in the incident aerodynamic flow [97]. Researchers have also explored the use of fluid–solid metamaterials for the manipulation of elastic wave propagation [95].

Other than the existing current methods, microfluidic techniques like microchannels developed using soft lithography can also be used to create space-coiling, circulating liquid, or other resonator-based acoustic metamaterials. In one of the works, a sub-wavelength meta-atom consisting of a resonant annular cavity biased by a circulating fluid, capable of producing giant acoustic nonreciprocity and acoustic isolation, was reported by Fleury et al. [98]. Using the concept of movement of fluid causing an angular momentum bias that splits the ring's azimuthal resonant modes, a linear, magnetic free circulator airborne for sound waves was developed to observe up to 40-decibel nonreciprocal isolation at audible frequencies.

## 5 Future perspective and conclusion

Even though fluidic actuation mechanisms have been well established for numerous lab-on-chip applications, their incorporation in diverse emerging fields like acoustic metamaterials has seldom been thoroughly investigated. This review highlights the recent developments of acoustic metamaterials design integrated with various microfluidic actuation mechanism.

Microfluidic works well in microscale regimes; thus, fabricating milli-metre or micron-sized active microfluidic designs supports their integration in the kHz to MHz AMM, respectively. It provides techniques to control and

automate the manipulation of liquid droplets, fluid streams, or bubbles in required arrangements with spatiotemporal precision. Fluid manipulation in acoustic metamaterials has shown promising capabilities, such as flexible integration, low power requirement, facile fabrication methods, and greater degree of freedom, while retaining soft and conductive/non-conductive properties of the metamaterials, which is not possible to achieve in solids. With this new amalgamation, the applications of acoustic wave steering, acoustic beam engineering, active tunability, and acoustic energy flow switch have been demonstrated surpassing the conventional metamaterials.

Even though much has been going on in building microfluidics-based metamaterial designs, however, in future, the limitations of liquid-based AMM like water droplet evaporation can be overcome by either utilising metal droplets or making a liquid reservoir on the AMM surface to provide liquid droplet on demand at the required position on the metamaterial [82]. Furthermore, the transparency of liquids like de-ionised water, alcohol, etc. allows for the integration of optical and acoustic designs for developing optoacoustic metamaterials in the future.

The recent advances of machine learning [99] and efficient optimization approaches [100] can also be integrated with fluidics-based AMM designs in the future to capture more details and features in an efficient fashion without expending on repetitive highly intensive time-consuming experimental processes.

**Data availability** All the data that support the findings of this study are included within the article.

**Open Access** This article is licensed under a Creative Commons Attribution 4.0 International License, which permits use, sharing, adaptation, distribution and reproduction in any medium or format, as long as you give appropriate credit to the original author(s) and the source, provide a link to the Creative Commons licence, and indicate if changes were made. The images or other third party material in this article are included in the article's Creative Commons licence, unless indicated otherwise in a credit line to the material. If material is not included in the article's Creative Commons licence and your intended use is not permitted by statutory regulation or exceeds the permitted use, you will need to obtain permission directly from the copyright holder. To view a copy of this licence, visit <http://creativecommons.org/licenses/by/4.0/>.

## References

1. N. Convery, N. Gadegaard, *Micro Nano Eng.* **2**, 76 (2019)
2. V. Ortseifen, M. Viefhues, L. Wobbe, A. Grünberger, *Front Bioeng. Biotechnol.* **8**, 1 (2020)
3. G.M. Whitesides, *Nature* **442**, 368 (2006)
4. X. Hou, Y. S. Zhang, G. T. De Santiago, M. M. Alvarez, J. Ribas, S. J. Jonas, P. S. Weiss, A. M. Andrews, J. Aizenberg, and A. Khademhosseini, *Nat Rev Mater* **2**, (2017).
5. A.G. Niculescu, C. Chircov, A.C. Bircă, A.M. Grumezescu, *Int. J. Mol. Sci.* **22**, 1 (2021)
6. S. Waheed, J.M. Cabot, N.P. Macdonald, T. Lewis, R.M. Guijt, B. Paull, M.C. Breadmore, *Lab Chip* **16**, 1993 (2016)
7. S. Patari, P. Datta, P.S. Mahapatra, *Sci. Rep.* **12**, 1 (2022)
8. S. Sachdeva, R.W. Davis, A.K. Saha, *Front Bioeng. Biotechnol.* **8**, 1 (2021)
9. C.D. Modak, A. Kumar, A. Tripathy, P. Sen, *Nat. Commun.* **11**, 4327 (2020)
10. N. Rastogi, P. Seth, R. Bhat, and P. Sen, *Anal Chim Acta* **1159**, (2021).
11. Y. Liu, X. Zhang, *Chem. Soc. Rev.* **40**, 2494 (2011)
12. J.E. Holliman, H.T. Schaeff, B.P. McGrail, Q.R.S. Miller, *Mater Adv* **3**, 8390 (2022)
13. M. Kadic, G.W. Milton, M. van Hecke, M. Wegener, *Nature Rev. Phys.* **1**, 198 (2019)
14. H.H. Huang, C.T. Sun, G.L. Huang, *Int. J. Eng. Sci.* **47**, 610 (2009)
15. S. H. Lee, C. M. Park, Y. M. Seo, Z. G. Wang, and C. K. Kim, *Phys Rev Lett* **104**, (2010).
16. W.J. Padilla, D.N. Basov, D.R. Smith, *Mater. Today* **9**, 28 (2006)
17. C. García-Meca, J. Hurtado, J. Martí, A. Martínez, W. Dickson, and A. V. Zayats, *Phys Rev Lett* **106**, (2011).
18. Y. Ding, Z. Liu, C. Qiu, and J. Shi, *Phys Rev Lett* **99**, (2007).
19. W. Zhang, Q. Song, W. Zhu, Z. Shen, P. Chong, D.P. Tsai, C. Qiu, A.Q. Liu, *Adv. Phys. X* **3**, 1417055 (2018)
20. J. Xu, R. Yang, Y. Fan, Q. Fu, F. Zhang, *Front. Phys.* **9**, 1 (2021)
21. C. Choi, S. Bansal, N. Münzenrieder, and S. Subramanian, *Adv Eng Mater* **23**, (2021).
22. S. Bansal, C. Choi, J. Hardwick, B. Bagchi, M.K. Tiwari, S. Subramanian, *Adv. Eng. Mater.* **25**, 2201117 (2023)
23. G. Memoli, M. Caleap, M. Asakawa, D.R. Sahoo, B.W. Drinkwater, S. Subramanian, *Nat. Commun.* **8**, 14608 (2017)
24. T.S. Kasirga, Y.N. Ertas, M. Bayindir, *Appl. Phys. Lett.* **95**, 3 (2009)
25. N.I. Zheludev, Y.S. Kivshar, *Nat. Mater.* **11**, 917 (2012)
26. K. Bi, Q. Wang, J. Xu, L. Chen, C. Lan, M. Lei, *Adv. Opt. Mater* **9**, 1 (2021)
27. S.K. Patel, Y. Kosta, *Microw. Opt. Technol. Lett.* **60**, 318 (2018)
28. Q. Zhao, L. Kang, B. Du, B. Li, J. Zhou, H. Tang, X. Liang, B. Zhang, *Appl. Phys. Lett.* **90**, 1 (2007)
29. F. Zangeneh-Nejad and R. Fleury, *Reviews in Physics* **4**, (2019).
30. G. Liao, C. Luan, Z. Wang, J. Liu, X. Yao, J. Fu, *Adv. Mater. Technol.* **6**, 1 (2021)
31. Q. Lu, X. Li, X. Zhang, M. Lu, Y. Chen, *Engineering* **17**, 22 (2022)
32. J. Zhang, B. Hu, and S. Wang, *Appl Phys Lett* **123**, (2023).
33. N. Gao, Z. Zhang, J. Deng, X. Guo, B. Cheng, and H. Hou, *Adv Mater Technol* **7**, (2022).
34. S. Laureti, D. A. Hutchins, L. A. J. Davis, S. J. Leigh, and M. Ricci, *AIP Adv* **6**, (2016).

35. D. Hutchins, P. Burrascano, L. Davis, S. Laureti, M. Ricci, *Ultrasonics* **54**, 1745 (2014)
36. G. Palma, H. Mao, L. Burghignoli, P. Göransson, and U. Iemma, *Applied Sciences (Switzerland)* **8**, (2018).
37. F. Li, R. Hu, *Sensors (Switzerland)* **21**, 1 (2021)
38. V. Arora, Y.H. Wijnant, A. De Boer, *Appl. Acoust.* **80**, 23 (2014)
39. R. Lathia, N. Sagar, and P. Sen, *European Physical Journal: Special Topics* **123**, (2022).
40. S.K. Cho, H. Moon, C.J. Kim, *J. Microelectromech. Syst.* **12**, 70 (2003)
41. J. Li and C.-J. “CJ” Kim, *Lab Chip* **20**, 1705 (2020).
42. Y. Zhang, N.T. Nguyen, *Lab Chip* **17**, 994 (2017)
43. N. Sagar, S. Bansal, and P. Sen, *Adv Mater Interfaces* **9**, (2022).
44. K.N. Nampoothiri, M.S. Seshasayee, V. Srinivasan, M.S. Bobji, P. Sen, *Sens Actuators B Chem* **273**, 862 (2018)
45. S. Bansal, Y. Tokuda, J. Peasley, S. Subramanian, *Langmuir* **38**, 6996 (2022)
46. S. Bansal, P. Sen, *Sens Actuators B Chem* **232**, 318 (2016)
47. Y. Zhang, Y. Liu, *Sensors & Diagnostics* **1**, 648 (2022)
48. E. Samiei, M. D. De Leon Derby, A. Van Den Berg, and M. Hoorfar, *Lab Chip* **17**, 227 (2017).
49. S. Bansal, P. Sen, *Langmuir* **33**, 11047 (2017)
50. K. N. Nampoothiri, M. S. Bobji, and P. Sen, *Int J Heat Mass Transf* **145**, (2019).
51. S. Yaman, M. Anil-Inevi, E. Ozcivici, and H. C. Tekin, *Front Bioeng Biotechnol* **6**, (2018).
52. K.N. Nampoothiri, N.S. Satpathi, A.K. Sen, *RSC Adv.* **12**, 23400 (2022)
53. J. Zhuang, J. Yin, S. Lv, B. Wang, Y. Mu, *Biosens. Bioelectron.* **163**, 112291 (2020)
54. V. Narayanamurthy, Z.E. Jeroish, K.S. Bhuvaneshwari, P. Bayat, R. Premkumar, F. Samsuri, M.M. Yusoff, *RSC Adv.* **10**, 11652 (2020)
55. D. Decrop, T. Brans, P. Gijzenbergh, J. Lu, D. Spasic, T. Kokalj, F. Beunis, P. Goos, R. Puers, J. Lammertyn, *Anal. Chem.* **88**, 8596 (2016)
56. D. Ozcelik, H. Cai, K.D. Leake, A.R. Hawkins, H. Schmidt, *Nanophotonics* **6**, 647 (2017)
57. S. Bansal, P. Sen, *J. Colloid Interface Sci.* **568**, 8 (2020)
58. A.M. Foudeh, D. Brassard, M. Tabrizian, T. Veres, *Lab Chip* **15**, 1609 (2015)
59. P. Qin, M. Park, K.J. Alfson, M. Tamhankar, R. Carrion, J.L. Patterson, A. Griffiths, Q. He, A. Yildiz, R. Mathies, K. Du, *ACS Sens* **4**, 1048 (2019)
60. A.R. Wheeler, H. Moon, C.J. Kim, J.A. Loo, R.L. Garrell, *Anal. Chem.* **76**, 4833 (2004)
61. M. B. Kulkarni and S. Goel, *Engineering Research Express* **2**, (2020).
62. R. Gaikwad, A.K. Sen, *Analyst* **146**, 95 (2021)
63. G. Narendran, S.Z. Hoque, N.S. Satpathi, K.N. Nampoothiri, A.K. Sen, *J. Micromech. Microeng.* **32**, 094001 (2022)
64. K. Mahesh, M. Varma, P. Sen, *Lab Chip* **20**, 4296 (2020)
65. N. Pamme, *Lab Chip* **7**, 1644 (2007)
66. P. Sajeesh, S. Manasi, M. Doble, A.K. Sen, *Lab Chip* **15**, 3738 (2015)
67. P. Sajeesh, A.K. Sen, *Microfluid Nanofluidics* **17**, 1 (2014)
68. A. Jagannath, H. Cong, J. Hassan, G. Gonzalez, M.D. Gilchrist, N. Zhang, *Biosens Bioelectron X* **10**, 100134 (2022)
69. Y. Li, X. Liu, Q. Huang, A.T. Ohta, T. Arai, *Lab Chip* **21**, 1016 (2021)
70. J.H. Lee, K.H. Lee, J.M. Won, K. Rhee, S.K. Chung, *Sens. Actuators A Phys.* **182**, 153 (2012)
71. Y. Xie, C. Zhao, *Nanoscale* **9**, 6622 (2017)
72. P. Rogers, A. Neild, *Lab Chip* **11**, 3710 (2011)
73. J.F. Louf, N. Bertin, B. Dollet, O. Stephan, P. Marmottant, *Adv. Mater. Interfaces* **5**, 1 (2018)
74. K. Khoshmanesh, A. Almansouri, H. Albloushi, P. Yi, R. Soffe, and K. Kalantar-Zadeh, *Sci Rep* **5**, (2015).
75. H. Ahmed, S. Ramesan, L. Lee, A. R. Rezk, and L. Y. Yeo, *Small* **16**, (2020).
76. A. Hashmi, G. Yu, M. Reilly-Collette, G. Heiman, J. Xu, *Lab Chip* **12**, 4216 (2012)
77. Anushka, A. Bandopadhyay, and P. K. Das, *Eur Phys J Spec Top* **232**, 781 (2023).
78. Z. Li, Z. Lin, L. Zeng, H. Wu, X.F. Zhu, *Front. Phys.* **10**, 1 (2022)
79. Z. Tian, C. Shen, J. Li, E. Reit, Y. Gu, H. Fu, S. A. Cummer, and T. J. Huang, *Adv Funct Mater* **29**, (2019).
80. N. M. Papadakis and G. E. Stavroulakis, *Applied Sciences (Switzerland)* **13**, (2023).
81. F. Langfeldt, H. Hoppen, W. Gleine, *Appl. Acoust.* **145**, 314 (2019)
82. S. Bansal, S. Subramanian, *Adv. Mater. Technol.* **6**, 2100491 (2021)
83. Z. Cai, S. Zhao, Z. Huang, Z. Li, M. Su, Z. Zhang, Z. Zhao, X. Hu, Y. S. Wang, and Y. Song, *Adv Funct Mater* **29**, (2019).
84. Z. Ma, H. Joh, D.E. Fan, P. Fischer, *Adv. Sci.* **9**, 1 (2022)
85. Z. Ma, K. Melde, A.G. Athanassiadis, M. Schau, H. Richter, T. Qiu, P. Fischer, *Nat. Commun.* **11**, 1 (2020)
86. D. Gritsenko, R. Paoli, *Appl. Sci. (Switzerland)* **10**, 1 (2020)
87. V. Leroy, A. Strybulevych, M. Lanoy, F. Lemoult, A. Tourin, J.H. Page, *Phys. Rev. B Condens Matter. Mater. Phys.* **91**, 1 (2015)
88. M. Lanoy, F. Lemoult, G. Lerozey, A. Tourin, V. Leroy, J.H. Page, *J. Appl. Phys.* **129**, 1 (2021)
89. Z. Huang, Z. Zhao, S. Zhao, X. Cai, Y. Zhang, Z. Cai, H. Li, Z. Li, M. Su, C. Zhang, Y. Pan, Y. Song, J. Yang, *ACS Appl. Mater. Interfaces* **13**, 53242 (2021)
90. D. Saintillan, *Annu. Rev. Fluid Mech.* **50**, 563 (2018)
91. Y.D. Liu, H.J. Choi, *Soft Matter* **8**, 11961 (2012)



92. J. De Vicente, D.J. Klingenberg, R. Hidalgo-Alvarez, *Soft Matter* **7**, 3701 (2011)
93. S. Chen, Y. Fan, Q. Fu, H. Wu, Y. Jin, J. Zheng, and F. Zhang, *Appl. Sci. (Switzerland)* **8**, (2018).
94. Z. Chen, C. Xue, L. Fan, S. Y. Zhang, X. J. Li, H. Zhang, and J. Ding, *Sci Rep* **6**, (2016).
95. Q. Zhang, K. Zhang, and G. Hu, *Appl. Phys. Lett.* **112**, (2018).
96. Muhammad, *Mater Today Commun* **32**, (2022).
97. F. Casadei and K. Bertoldi, *J. Appl. Phys.* **115**, (2014).
98. R. Fleury, D. L. Sounas, C. F. Sieck, M. R. Haberman, and A. Alù, *Science (1979)* **343**, 516 (2014).
99. Muhammad, J. Kennedy, and C. W. Lim, *Mater. Today Commun.* **33**, 104606 (2022).
100. P. Mittal, K. Mitra, *IFAC-PapersOnLine* **50**, 159 (2017)